A R C H I V E S O F M E T A L L U R G Y A N D M A T E R I A L S
Volume 54 2009 Issue 3

P. LACKI*

NUMERICAL ANALYSIS OF THE VOID EVOLUTION DURING METAL PLASTIC DEFORMATION

ANALIZA NUMERYCZNA EWOLUCJI NIECIĄGŁOŚCI MATERIAŁOWEJ PODCZAS DEFORMACJI PLASTYCZNEJ

Quality of the die forgings essentially depends on the material defects (voids) and possibilities of their correction during the forging process. Material defects cause unfavourable plastic strain distribution in the forging volume. In case of precise forging the defects also have impact on the precision of forging geometry. In the paper a numerical simulation of the material void influence on the die forging process has been presented. Two first operations of the die forging process, i.e. upsetting and preparing have been analysed. Numerical calculations have been made with the ADINA System based on the Finite Element Method. Elastic properties of the dies made from hot-work tool steel and elastic-plastic properties of the deformed material (ŁH15 bearing steel) have been assumed in the numerical model. For the sake of axial symmetry the model has been simplified. On the basis of numerical simulation analysis the possible way of solving some problems occurring during design of die forging process will be presented.

Keywords: defects, die forging, numerical simulation

Jakość odkuwek matrycowych w dużej mierze zależy od występujących defektów (nieciągłości) materiałowych i możliwości ich korekcji podczas procesu kucia. Nieciągłości materiałowe wywołują niekorzystny rozkład odkształceń plastycznych w objętości odkuwki. W przypadku kucia dokładnego wady materiałowe mają również wpływ na dokładność geometrii odkuwki. W artykule zaprezentowano symulację numeryczną wpływu nieciągłości materiałowej na proces kucia. Przeanalizowano dwie pierwsze operacje kucia tj. spęczanie i kucie wstępne. Obliczenia numeryczne wykonano za pomocą programu ADINA System opartego na metodzie elementów skończonych. W modelu numerycznym przyjęto właściwości sprężyste dla materiału matrycy, wykonanej ze stali narzędziowej do pracy na gorąco oraz sprężysto-plastyczne dla materiału odkuwki (stal łożyskowa ŁH15). Ze względu na osiową symetrię modelu przyjęto pewne uproszczenia. Na podstawie analizy symulacji numerycznej przedstawiono możliwości rozwiązywania niektórych problemów występujących podczas kucia matrycowego.

1. Introduction

The growing demands for high quality products forces forgings producers to put more emphasis on the quality aspects and fulfilment of the ISO standard requirements. Such a situation increases the effort spent on identification of defects and explanation of their causes. Quality of the die forgings essentially depends on the material defects and possibilities of their correction during the forging process. The characteristic longitudinal and transverse cracks are the most often defects arising during solidification and cooling of ingot. The cracks result from shrinkage stresses exceeding steel strength. Analysis of causes and effects of the defects poses a complex problem. Predictions how the material void will behave during forming process is especially difficult. Material defects (voids) can cause unfavourable plastic strain distribution in the forging volume. In case of precise forging the defects also have impact on the precision of forging geometry. Figure 1, for example, shows a material discontinuity defect.

Fig. 1. An example of material discontinuities

* CZĘSTOCHOWA UNIVERSITY OF TECHNOLOGY, INSTITUTE OF METAL FORMING, QUALITY ENGINEERING AND BIOENGINEERING, 42-200 CZĘSTOCHOWA, 21 ARMII KRAJOWEJ AV., POLAND

In the paper an attempt has been made to assess the possibilities of simulation and prediction of the results of the material void during precise forging process. The numerical simulation results of void evolution during plastic deformation of ŁH15 bearing steel in two forging operations have been presented. On the basis of numerical simulation analysis of the die forging process, taking into account material defects, the possible way of solving the problems occurring during design of die forging process was presented.

2. Numerical model

A rolling bearing, shown in Figure 2 was analysed in the numerical simulation. Two first forging operations, i.e. upsetting and preparing were modelled. Numerical calculations had been made with the ADINA System using Finite Element Method. Figure 3 shows the numerical model of the upsetting process. For the sake of an axial symmetry of the problem 2D axial-symmetrical model of the process has been assumed. Numerical model had 19614 nodes and 4752 square 8-node elements.

Fig. 2. A view of the analysed rolling bearing

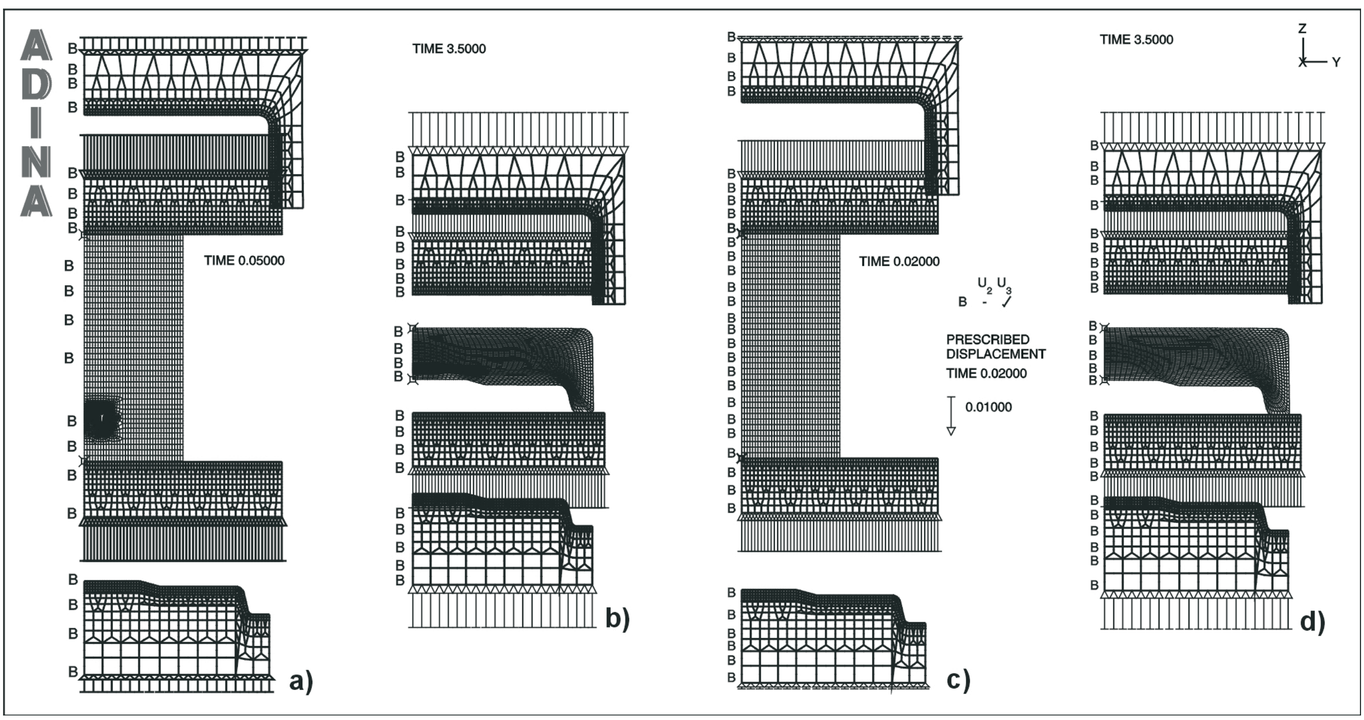

Fig. 3. MES numerical model; a) the forging with a defect before deformation, b) the forging with a defect after deformation, c) the forging with no defect before deformation, d) the forging with no defect after deformation

Two following variants of the forging process were analysed: forging without any defects and forging with a defect. Figure 2a) and 2b) present the finite element mesh for the tools and forging with the defect, adequately, before and after the forging process while Figure 2c) and 2d) present the finite element mesh for the forging without any defect. An isothermal course of the process and Coulomb frictional model on the contact surface between the forging and tools have been assumed. Friction coefficient was $\mu = 0.2$. The same frictional model but friction coefficient $\mu = 0.25$ were assumed for the contact zone between defect surfaces. The tool was made from WCL hot-work tool steel and the forging was made from ŁH15 bearing steel.

TABLE 1
Chemical constitution of the materials

	chemical constitution [%]						
	C	Mn	Si	Cr	Mo	V	Fe
Tool [WCL]	0.4	0.4	1.0	5.0	1.3	0.3	balance
Forging [ŁH15]	0.95-1.1	0.25-0.45	0.15-0.35	1.3-1.65	–	–	balance

Though the real material defects are irregular, in the simulation material discontinuity was modelled as a three-pointed star (see Fig. 4) with the arms directed at the angle of 0, 45 and 90° to the direction of the tool motion. Such a defect location allows investigating the results of the forging process depending on the defect position in the slug forging. In order to better calculation precise the finite element mesh was thickened in the area of the defect (in places its initial shape was irregular).

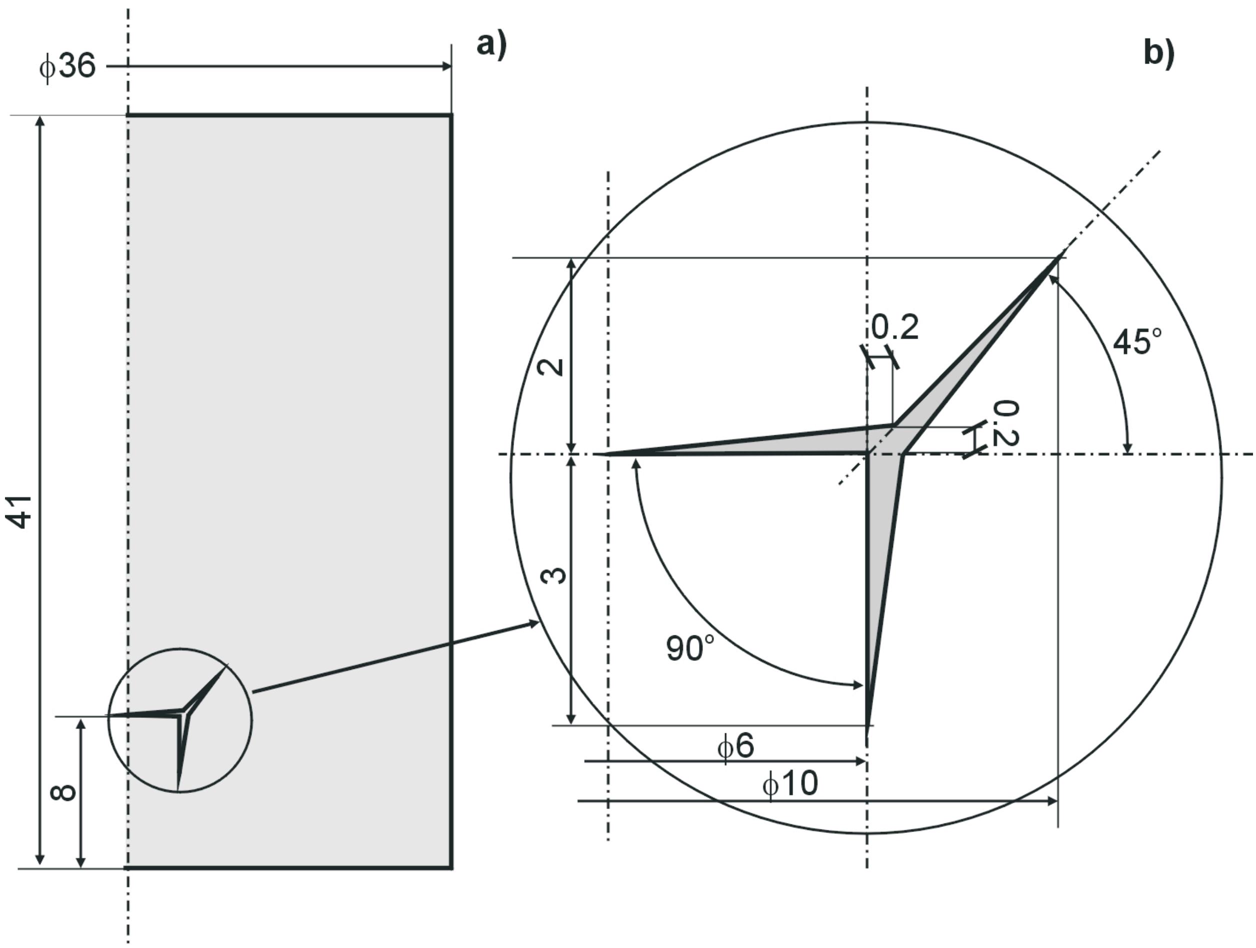

Fig. 4. Defect geometyry: a) a location of the defect in the slug forging, b) defect dimendions [mm]

3. Calculation results and discussion

Figures 5, 6, and 7 show defect geometry after the subsequent forging operations with the marked lines of material flow in the defect area. Figure 5a shows a tool position in relation to the forging in t=0s. The defect outline was marked schematically. Figure 5b shows the initial lines of the material flow. A, B, C letters describing the characteristic areas and A_1, A_2, B_1, B_2, C_1, C_2 ones describing the appropriate edges were introduced in order to better description of changes occurring in the defect area.

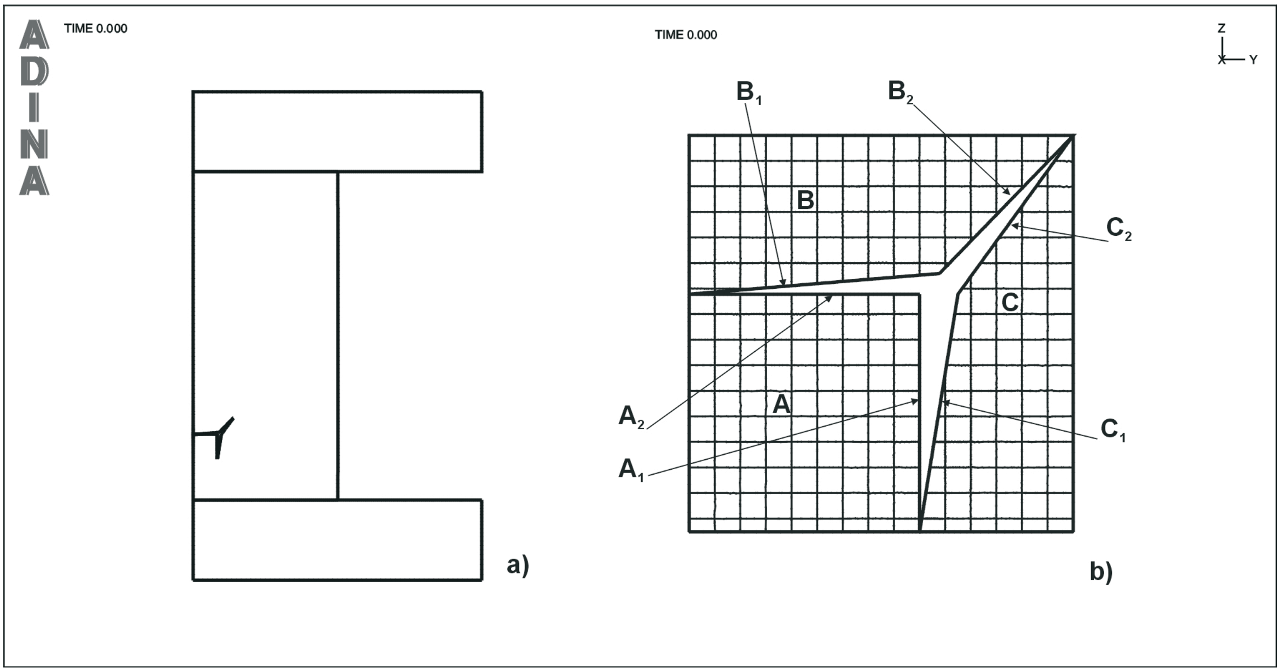

Fig. 5. An initial geometry of the defect: a) scheme of the deformation with a defect, b) lines of the material flow in the defect area

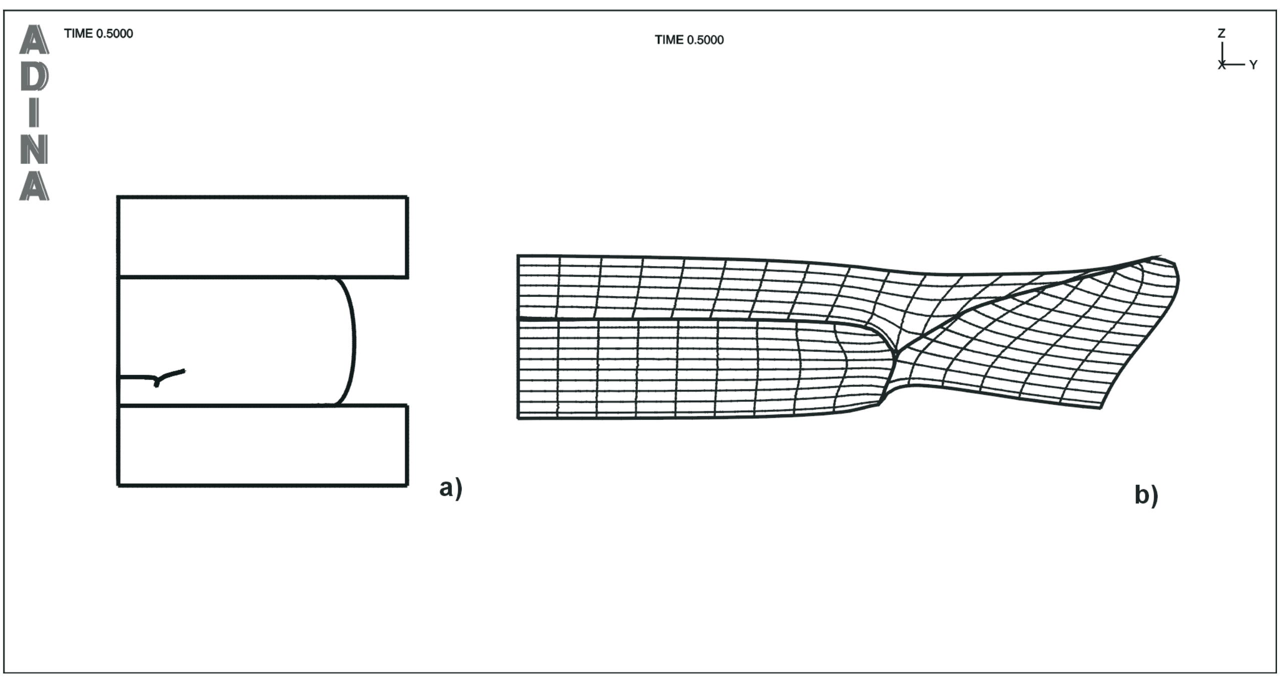

Fig. 6. Defect geometry after upsetting operation t = 0.5s; a) scheme of deformation with the defect b) material flow lines in the defect area

Upsetting of the slug forging to the height of h=16mm is the first operation of the analysed process. During this operation the defect closes. The individual defect surfaces get contact and void disappear. Strain scheme and defect geometry after upsetting operation were shown in Figure 6. *A* area joins to *C* area by A_1 and C_1 surfaces. *C* area joins to *B* area by C_2 and B_2 surfaces. *B* area joins to *A* area by A_2 and B_1 surfaces. In the defect area there is a clear deformation of the flow lines caused by material discontinuity. The defect affects *A* area slightly. Flow lines are slightly disrupted in the distant part from the symmetry axis. *B* area shows some regularity in flow in the contact zone with *A* area, while the strongest disruption appears in the contact zone with *C* area. Material discontinuity affects *C* area mostly. The defect was closed as a result of upsetting process. The initial three star arms transform into three lines. A direction of the horizontal line, which has arisen from combination of A_2 and B_1 lines, changes slightly with relation to the initial state. There is an increase in length in Y direction and the line curves slightly in the most distant section from the symmetry axis. The defect arm with the initial slope of 45° lengthens and the slope is of 30°. A vertical defect arm shortens and gets out of plumb in Y direction.

At the end of the die forging process there is an increase in stresses both in the die and forging [8.9]. Such stress increase can lead to the stable closure of the defect. There is no any literature report giving conditions when the stable closure of the defect appears. In practice it is known that closure of the defects with oxidizing surfaces is more difficult.

In the paper it was assumed that the defect does not close and the defect surfaces can shift along themselves.

In Figure 7 the flow lines after the preparing operation were shown. Deformation in the area of material discontinuity grows as a result of a higher deformation degree. There is a further elongation of A_2-B_1 and C_2-B_2 lines. A_1-C_1 line disappears after the second operation. B area fulfils the space between A_1-C_1 lines splitting up A and B areas.

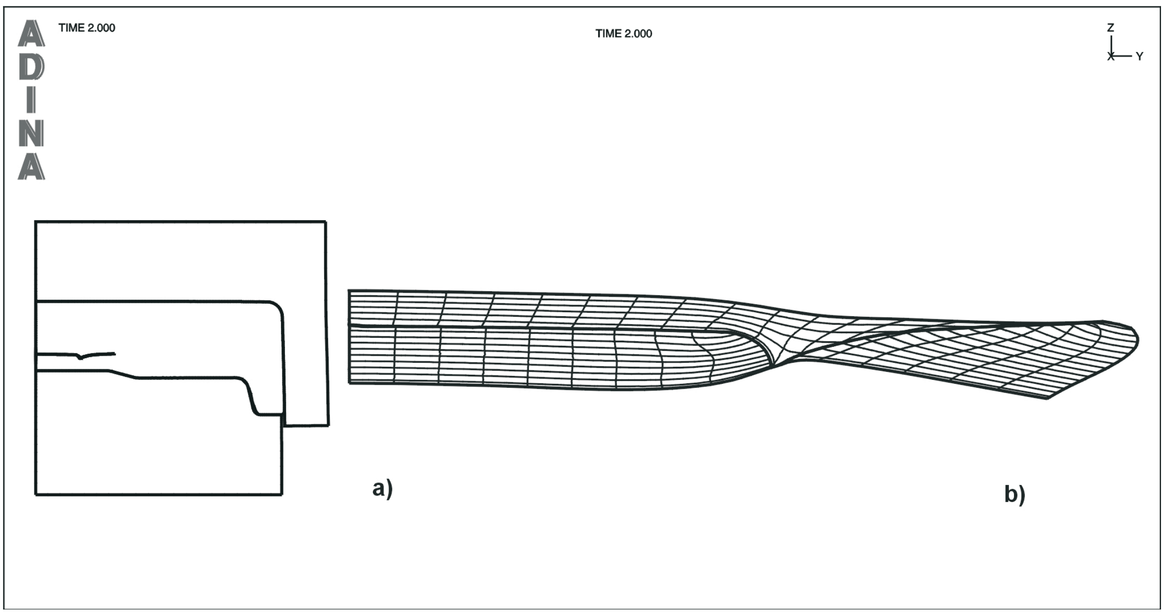

Fig. 7. Defect geometry after the preparing operation t = 2s; a) strain scheme with the defect, b) the material flow lines in the defect area

Figure 8 and 9 show the defect development during further deformation. Detailed observation of changes in material deformation allows assessing the defect effect better. Figure 8 shows plastic strain distribution in the defect area during the first forging operation.

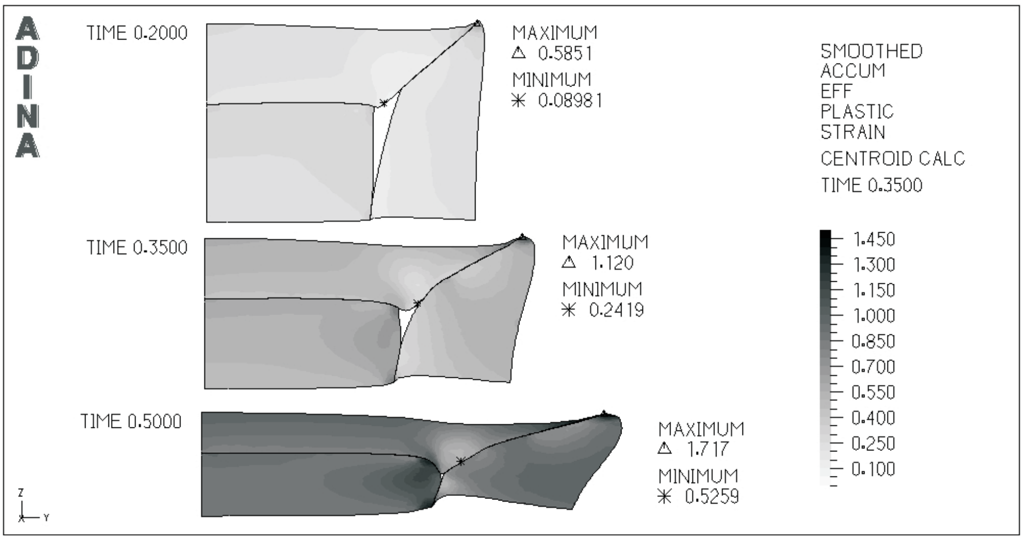

Fig. 8. Change in plastic strains in the defect area during upsetting

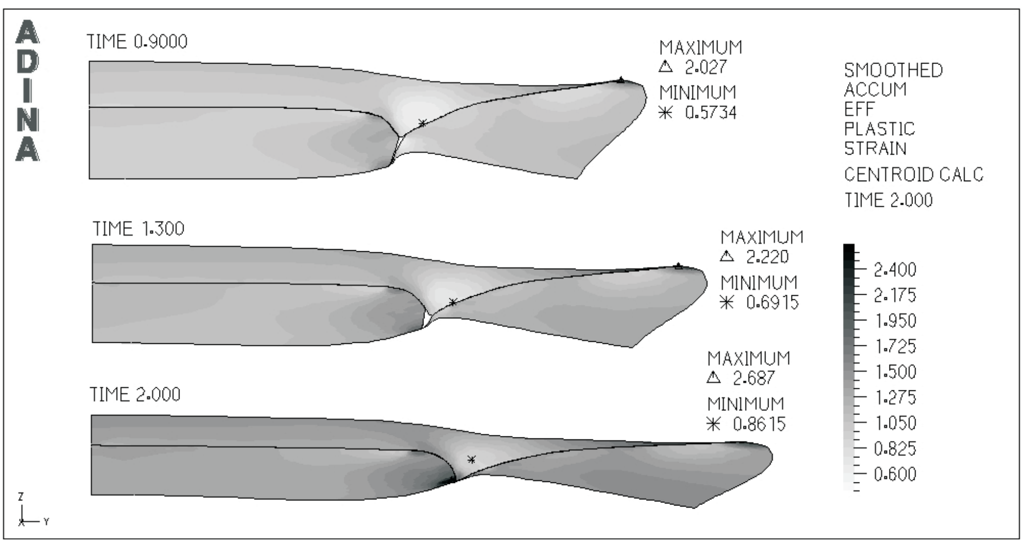

Fig. 9. Plastic strain change in the defect area during preparing operation

In the figure the results for three upsetting stages t_1=0.2s, t_2=0.35s, and the final time t_3=0.5s have been given. At t_2 time the closure of the horizontal and slope arms is observed. The vertical arm closes gradually. A part of the space between *A* and *C* area is fulfilled by *B* area till the hole closure. Value of plastic strains in the defect area increases gradually. Maximal strains occur in the upper right corner of *C* area while the lowest ones are in the bottom right corner of *B* area. Maximal strain value after upsetting operation is ε=1.71 and minimal one is ε=0.52. Strains are no uniform so it can affect changes in mechanical properties in this area.

In the vicinity of the symmetry axis strains are more uniform. The most differences in local strain values concentrate around the vertical arm of the defect. Similar character of plastic strain also occurs in the second forging operation. The location of the minimal and maximal strains does not change essentially but their values rise considerably. The maximal strain value after preparing operation is ε=2.68 and the minimal one is ε=0.86. Figure 9 shows development of the defect surface during the second operation. Repeated creation of the defect (material discontinuity) is characteristic for this forging stage. Some part of *B* area under the outer conditions moves along the vertical defect arm and the defect opens again. In the last stage of the preparing operation *B* area fulfils the void and the defect closes. During this process the local maximal strain appears in the bottom right corner of *A* area. Such high increase in strain can cause a crack and further development of the defect.

Material discontinuity not only does cause a local change in strain distribution but also changes plastic strain in the whole forging volume. Figure 10 and 11 present plastic strain distribution in a section of the forging and geometry of the contact surface between the tool and forging after the second forging cycle. Material discontinuity, which is visible in Figure 10 in comparison with the forging without any defect, causes decrease in strain value in the area between the lower die and the line of the defect closure. The maximal strain value in the forging without any defect is ε_{max}=2.68. Material discontinuity causes increase in maximal strain value of about 30%, which localises in the area of a concave radius of the forging. The defect contributes to a change of the maximal value location. During deformation of the material without any defects maximal value localises in a distance from the concave forging radius. The defect affects dislocation of maximal strain towards the surface. High strain values occur along the generating line of the concavity. The outer dimensions of the slug forging were the same for the case with and without the defect. A difference in volume being a result of the material discontinuity affects an underfill of the die, what is seen in Figure 10.

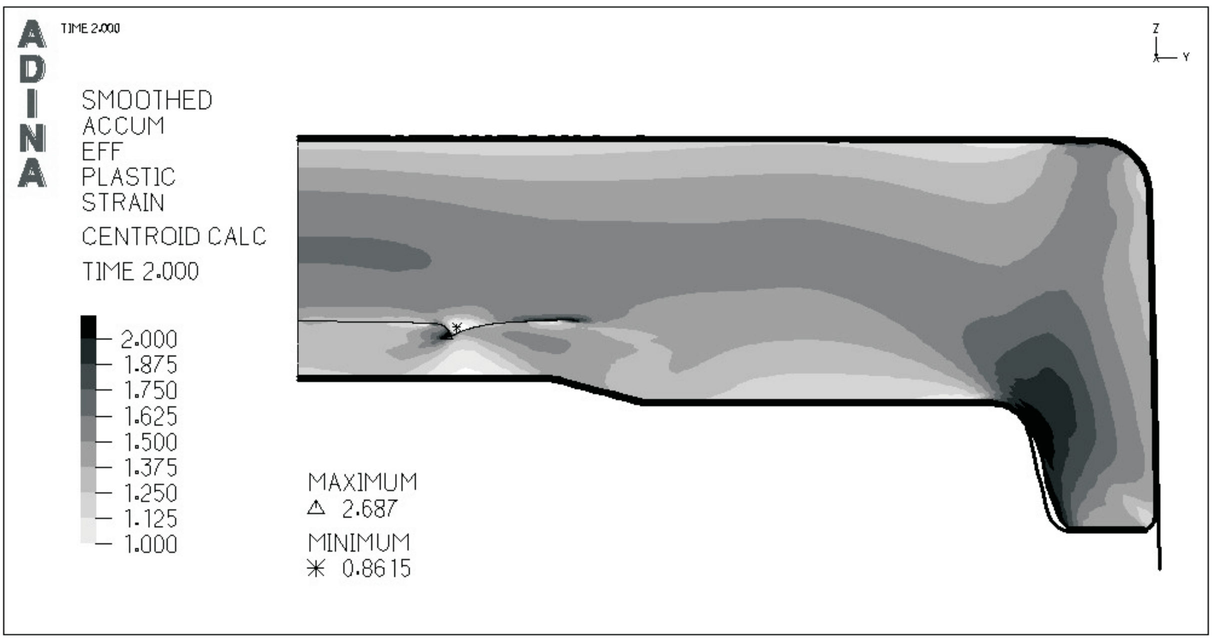

Fig. 10. Plastic strain distribution in the forging with the defect after the second forging cycle

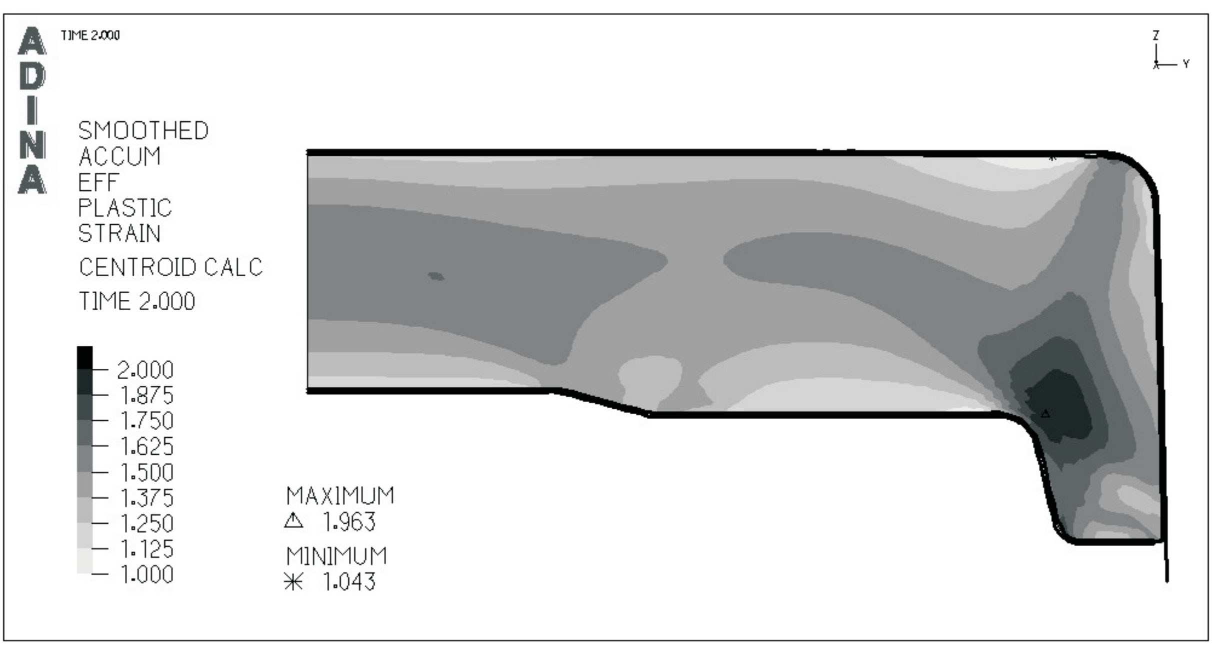

Fig. 11. Plastic strain distribution in the forging without any defects after the second forging cycle

4. Conclusions

The calculations allow assessing the effects of material discontinuity in the forging. According to the numerical simulation analysis of the die forging process it is possible to draw the following conclusions:

1. Material discontinuity depending on deformation conditions can close and open again during the forging process. The defect surfaces move relatively to each other during the whole forging cycle. Depending on the initial defect geometry there is a change in length of surfaces, which create the defect. In the analysed case the horizontal defects lengthen while vertical ones shorten.
2. In the defect area a relative extreme of plastic strain appears. High strain values in the zone of sharp defect edge can be extremely dangerous. It can lead to the further development of the defect.
3. Material discontinuity affects changes in strain state in the forging. It results in decrease of the strain value in the zone under the line of defect closure respecting the forging with no defect and increase of maximal strain values.
4. Numerical simulations allow exploring and analysing technological processes. The proper technology allows obtaining the products of better quality.

Acknowledgements

Financial support of Structural Funds in the Operational Programme – Innovative Economy (IE OP) financed from the European Regional Development Fund – Project No POIG.0101.02-00-015/08 is gratefully acknowledged.

Received: 20 May 2009.

REFERENCES

[1] P. Wasiunyk, Kucie matrycowe. Warszawa: WNT, 1987.

[2] Z. Krzekotowski, Technologia kucia swobodnego i półswobodnego. Poland Katowice: Wydawnictwo „ŚLĄSK", 1964.

[3] AV. Kutyskin, Veroatnostnaa ocenka vozniknovenia defektov pri obrezke obloa i probivke peremycki osesimmetricnych pokovok. Kuzn.-stampov. Proiz. **43**, 9 (2001).

[4] J. Adamus, M. Gierzyńska-Dolna, P. Lacki, Kompleksowe sterowanie jakością odkuwek matrycowych. Obróbka Plastyczna, 2001. [5] Ohasi T, Motomura M. Expert system of cold forging defects using risk analysis tree network with fuzzy language. J. Mat. Proc. Technol. **107**, 1-3 (2000).

[5] R. Balendra, Y. Qin, Identification and classification of flow-dependent defects in the injection forging of solid billet. J. Mat. Proc. Technol. **106**, 1-3 (2000).

[6] J. Radecki, E. Łabuda, Symulacja zmian objętości nieciągłości materiałowych w czasie odkształcenia plastycznego. Materiały VI Konferencji pt. Zastosowanie Komputerów w Zakładach Przetwórstwa Metali. KomPlasTech'99. Poland-Szczyrk, 1999.

[7] R. Szyndler, J. Sińczak Wpływ konstrukcji matryc na dokładność wykonania odkuwek. Materiały konferencji QUALITY 2001 Inżynieria Jakości w Technikach Wytwarzania. Częstochowa, 2001.

[8] J. Sińczak, A. Łukaszek, Obciążenie narzędzi przy kuciu wielokrotnym pierścieni łożysk tocznych. Obróbka Plastyczna Metali **12**, 3 (2001).